

# **An Investigation of the Impedance Rise and Power Fade in High-Power Li-Ion Cells \***

Ira Bloom, Scott Jones, Vincent Battaglia, and Gary Henriksen  
Electrochemical Technology Program  
Argonne National Laboratory  
9700 South Cass Avenue  
Argonne, IL 60439-4837 USA

Chester Motloch, Jon Christophersen, and Jeffrey Belt  
Idaho National Engineering and Environmental Laboratory  
P.O. Box 1625  
Idaho Falls, ID 83415

Rudolph Jungst, Herbert Case, and Daniel Doughty  
Sandia National Laboratory  
P.O. Box 5800  
Albuquerque, NM 87185

To be presented at the  
19<sup>th</sup> International Electric Vehicle Symposium (EVS-19)  
The Answer for Clean Mobility  
Busan, South Korea  
October 19-23, 2002

The submitted manuscript has been created by the University of Chicago as Operator of Argonne National Laboratory ("Argonne") under Contract No. W-31-109-ENG-38 with the U.S. Department of Energy. The U.S. Government retains for itself, and others acting on its behalf, a paid-up, nonexclusive, irrevocable worldwide license in said article to reproduce, prepare derivative works, distribute copies to the public, and perform publicly and display publicly, by or on behalf of the Government.
---

---

\*This work was performed under the auspices of the U.S. Department of Energy, Office of Advanced Automotive Technologies, under Contract No. W-31-109-Eng-38.

# An Investigation of the Impedance Rise and Power Fade in High-Power, Li-Ion Cells

Ira Bloom, Scott A. Jones, Vincent S. Battaglia, Edward G. Polzin, Gary L. Henriksen, Chester G. Motloch, Jon P. Christophersen, Jeffrey R. Belt, Chinh D. Ho, Randy B. Wright, Rudolph G. Jungst, Herbert L. Case, and Daniel H. Doughty

## Abstract

Two different cell chemistries, Gen 1 and Gen 2, were subjected to accelerated aging experiments. In Gen 1 calendar life experiments, useful cell life was strongly affected by temperature and time. Higher temperature accelerated cell performance degradation. The rates of impedance increase and power fade followed simple laws based on a power of time and Arrhenius kinetics. The data have been modeled using these two concepts, and the calculated data agree well with the experimental values.

The Gen 1 calendar life increase and power fade data follow  $(\text{time})^{1/2}$  kinetics. This may be due to solid electrolyte interface (SEI) layer growth. From the cycle life experiments, the impedance increase data follow  $(\text{time})^{1/2}$  kinetics also, there is an apparent change in overall power fade mechanism, from 3% to 6%  $\Delta\text{SOC}$ . Here, the power of time changes to a value less than 0.5 indicating that the power fade mechanism is due to factors more complex than just SEI layer growth.

The Gen 2 calendar and cycle life experiments show the effect of cell chemistry on kinetics. The calendar life impedance data follow either “linear” or  $(\text{time})^{1/2}$  plus linear kinetics, depending on time and temperature. *Copyright © 2002 EVS19*

**Keywords:** battery, lithium ion, cycle life, battery model

## 1. Introduction

Lithium-ion rechargeable batteries have attracted the interest of many research groups and industries. Typically, these batteries consist of lithiated-carbon intercalation anodes, a liquid organic electrolyte containing a lithium salt, and a lithium insertion cathode (usually  $\text{Li}_x\text{NiO}_2$ ,  $\text{Li}_x\text{CoO}_2$  or  $\text{Li}_x\text{Mn}_2\text{O}_4$ ). In its goal of developing an 80-mpg vehicle, the FreedomCAR Partnership is focusing its energy storage R&D efforts on high-power lithium-ion batteries to meet its energy storage requirements for leveling the load on a prime power source and for capturing regenerative braking energy. Industrial developers have demonstrated that the lithium-ion battery technology is capable of meeting the performance and cycle life requirements for this application, but barriers to commercialization remain. They are calendar life, thermal abuse tolerance and safety.

The U.S. Department of Energy established the Advanced Technology Development (ATD) Program to address key issues limiting the life and safety of high-power Li-ion batteries. In this program, three national laboratories, Argonne National Laboratory (ANL), Idaho National Engineering and Environmental Laboratory (INEEL) and Sandia National Laboratories (SNL), are working to develop an understanding of the effect of accelerated calendar and cycle life testing on the performance of Li-ion cells, especially on the impedance and power of the cells.

This experimental effort used two different Li-ion cell chemistries in 18650-size packages. The cells were built to ANL’s specifications. The Gen 1 cells used the best commercially available cell chemistry at the time of construction. The Gen 2 cells used materials that were either developed in the ATD Program or selected based on extensive screening of the most advanced materials that could be obtained worldwide.

The Gen 1 calendar and cycle life experiments used a complete factorial matrix. Using the results from the Gen 1 cells, we were able to model the changes in impedance and power with time. The modeling helped elucidate the types of fade mechanisms present. The Gen 2 experiments were much more limited. Using just three temperatures, we were able to learn much about the degradation processes at work and how they are affected by cell chemistry.

## 2. Experimental

The experimental conditions and results for the Gen 1 work have been presented elsewhere [1]. Briefly, the exact compositions of the Gen 1 and Gen 2 cells are given in Tables 1 and 2, respectively.

Table 1. Gen 1 Cell Chemistry

Positive Electrode: 8 wt% PVDF binder 4 wt% SFG-6 graphite 4 wt% carbon black 84 wt% $\text{LiNi}_{0.8}\text{Co}_{0.2}\text{O}_2$	Negative Electrode: 9 wt% PVDF binder 16 wt% SFG-6 graphite 75 wt% MCMB-6 graphite
Electrolyte: 1M $\text{LiPF}_6$ in EC/DEC (1:1 by wt)	Separator: 37- $\mu\text{m}$ -thick PE Celgard separator

For Gen 1, the cathodes and anodes were cast as thin films on aluminum and copper foils, respectively, to yield an effective active area of  $\sim 678 \text{ cm}^2$ . After assembly, the cells underwent a few formation cycles and a 21-day stand before shipping to the test laboratories. For Gen 2, the cathodes and anodes were cast as thin films on aluminum and copper foils, respectively, to yield an effective active area of  $\sim 846 \text{ cm}^2$ .

Table 2. Gen 2 Cell Chemistry

Positive Electrode: 8 wt% PVDF binder 4 wt% SFG-6 graphite 4 wt% carbon black 84 wt% $\text{LiNi}_{0.8}\text{Co}_{0.15}\text{Al}_{0.05}\text{O}_2$	Negative Electrode: 8 wt% PVDF binder 92 wt% MAG-10 graphite
Electrolyte: 1.2 M $\text{LiPF}_6$ in EC/EMC (3:7 by wt)	Separator: 25- $\mu\text{m}$ -thick PE Celgard separator

In the Gen 1 aging studies, three to six cells were used at each condition. The calendar-life study using the Gen 1 cells was a complete factorial matrix that consisted of four temperatures (40, 50, 60, and 70°C) and three states of charge (SOC, 40, 60 and 80%). These SOC's correspond to room temperature OCVs of 3.600, 3.747 and 3.918 V, respectively, as determined from C/25 discharge tests. Additional information was gathered during the soak periods at temperature. Because of different equipment at the three test laboratories, two types of calendar life tests were performed. ANL measured the leakage current (group A). SNL and INEEL conducted the pulse-per-day calendar test (group B) [2].

The cycle-life study using the Gen 1 cells was also a complete factorial matrix. In addition to the parameters mentioned for the calendar-life work, two  $\Delta\text{SOCs}$  (3 and 6%, given in Figs. 1 and 2) were used [2].

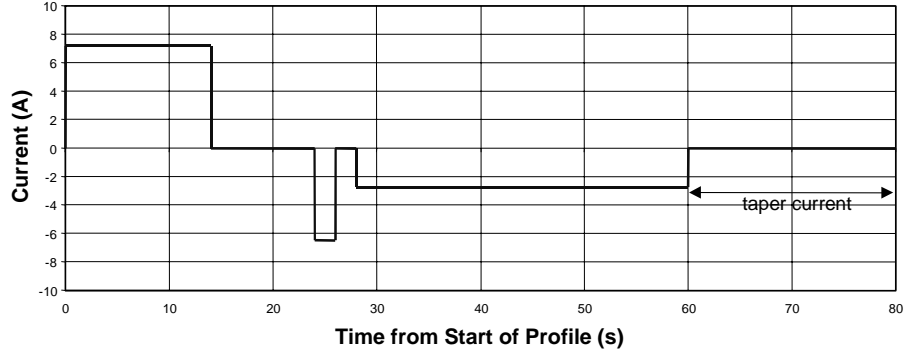


Fig. 1. Profile for 3%  $\Delta$ SOC.

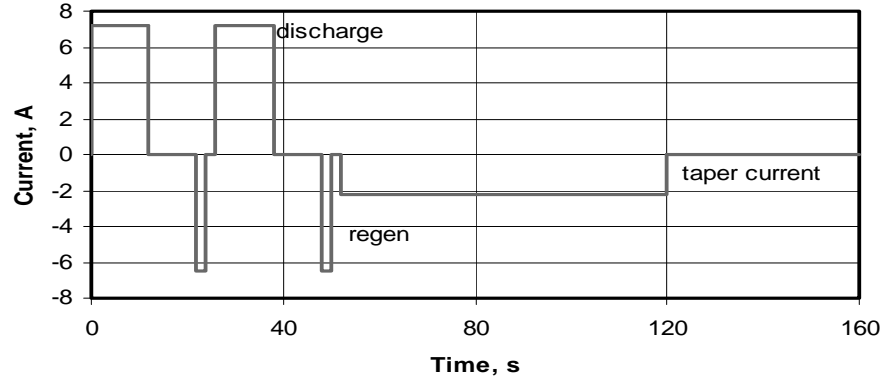


Fig. 2. Profile for 6%  $\Delta$ SOC.

The calendar-life study using the Gen 2 cells was more limited. It consisted of aging the cells at 45 and 55°C at 60% SOC (3.723 V at room temperature). The pulse-per-day calendar test was used at ANL. The cycle-life study consisted of aging the cells at 45 and 25°C using a scaled 25-Wh PNGV profile [3] at INEEL.

For both Gen 1 and Gen 2, each cell was characterized by the hybrid pulse power characterization test (HPPC) [4]. After 4 weeks at the desired temperature (2 weeks for the cells at 70°C), changes in cell performance were gauged by cooling the cells down and repeating the HPPC test at 25°C. For Gen 1 and Gen 2 cells, power change was determined at 60% SOC.

Cell end-of-life was performance based. If the cell could not perform the 6<sup>th</sup> HPPC pulse within its voltage window, the cell had reached the end-of-life criterion.

The detailed analysis of HPPC data to derive impedance and power is given in references 1, 4 and 5 and will not be given here. All further analyses focus on changes in discharge impedance and power.

The derived values at 60% SOC were pooled and averaged. They were used in curve fitting experiments to elucidate temperature- and time-dependencies. For the Gen 1 cell data, the data could be fit to the general equation

$$Q = A \exp(-E_a/RT) t^z, \quad (1)$$

where  $Q$  is the impedance or power change,  $A$  the pre-exponential factor,  $E_a$  the activation energy in J,  $R$  the gas constant,  $T$  the absolute temperature,  $t$  the time, and  $z$  the exponent of time. This equation was linearized by taking the natural logarithm of both sides of the equation and using the Microsoft EXCEL function LINEST to calculate  $\ln A$ ,  $E_a/R$ , and  $z$ . In addition, LINEST returned the standard error (SE) around each parameter and the regression coefficient,  $r^2$ .

No temperature dependency was calculated from the Gen 2 data since only two temperatures were used for each aging condition. The data were curve fit using the general expression

$$Q = f(t), \quad (2)$$

where  $f(t)$  is  $at$  or  $at^{1/2}$  ( $a$  is a constant) and  $r^2$  is monitored to identify the best fit.

### 3. Results and Discussion

For clarity, the results and discussion for Gen 1 and Gen 2 are presented separately.

#### 3.1. Gen 1

In general, the cells at higher temperatures reached end-of-life before the ones at lower temperatures. For example, in both the calendar and cycle life tests, the 70°C cells failed after 2 weeks of testing. The ones at 60°C tended to fail after 4 weeks of testing. In addition to the temperature effect on life, cycling the cells and pulsing them during the calendar test tended to shorten their lives. Premature cell failure and cell leakage produced a sparse data matrix to analyze. The initial average values for the cell populations are given in Table 3. The average error around these values is 5 to 7%.

Table 3. Initial Average Values from Cells in this Study

Test / Group	Impedance, mΩ	Power, W
80% calendar life	73.3	43.8
60% calendar life (A)	65.9	45.9
60% calendar life (B)	73.9	30.1
40% calendar life	66.8	46.3
Cycle life (all SOC's and ΔSOC's)	59.1	36.1

Note: 80, 60 and 40% indicate the SOC. (A) indicates cells monitored for leakage current. (B) indicates cells subject to one current pulse per day.

##### 3.1.1. Calendar Life

Typical impedance versus SOC (as given by the cell voltage, 60% = 3.747 V OCV) and power versus SOC curves are given in Figs. 3 and 4. The curves in these figures show the expected trends: impedance increases with time and power density decreases with time.

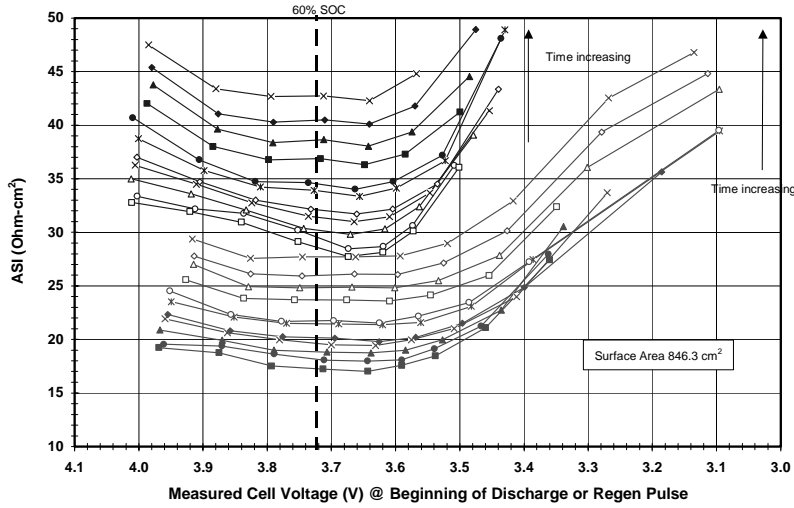


Fig. 3. Typical HPPC-derived impedance vs. cell voltage data. The top set of curves are from discharge and the bottom, from regen. These curves represent data spanning 40 weeks.

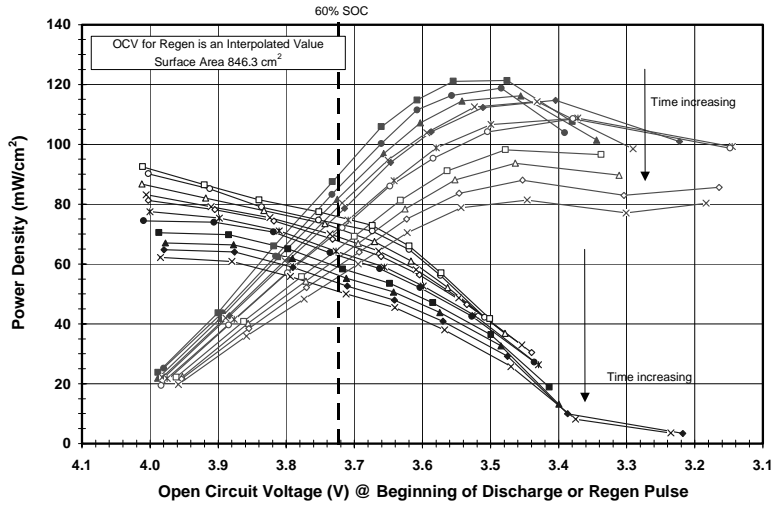


Fig. 4. Typical HPPC-derived Power Density vs. Cell Voltage curves. The top set of curves are from discharge and the bottom, from regen. These curves represent data spanning 40 weeks.

The parameters from all the fits are given in Table 4 for the three SOC's. The cells exposed to 70°C and 80% SOC failed very quickly. Very few impedance and power data were obtained under these conditions; these cells were excluded from further analysis. Table 4 also contains the fitting results using the remaining temperature data at 40, 50 and 60°C. The values of  $r^2$  show that most of the fits are very good and the data followed square-root-of-time and Arrhenius kinetics.

Plots containing example impedance and power change are given in Figs. 5 and 6. In these plots, markers represent the experimental values and the calculated values are represented by curves.

Table 4. Impedance Change and Power Fade Fitting Parameters

% SOC		Impedance Increase				Power Fade			
		z	Ea/R, K	lnA	r <sup>2</sup>	z	Ea/R, K	lnA	r <sup>2</sup>
40	Value	0.52	6827.30	23.1	0.98	0.44	6095.95	20.83	0.97
	Std. Error	0.05	350.94	1.04		0.06	423.05	1.25	
60 / A	Value	0.51	6810.67	23.49	0.99	0.46	5541.28	19.36	0.81
	Std. Error	0.06	374.31	1.11		0.18	1086.14	3.21	
60 / B	Value	0.51	4828.96	17.50	0.94	0.41	3820.41	14.31	0.93
	Std. Error	0.16	759.73	2.18		0.13	636.16	1.83	
80	Value	0.61	2715.18	10.74	0.87	0.46	2262.09	9.47	0.83
	Std. Error	0.14	719.42	2.18		0.15	750.39	2.27	

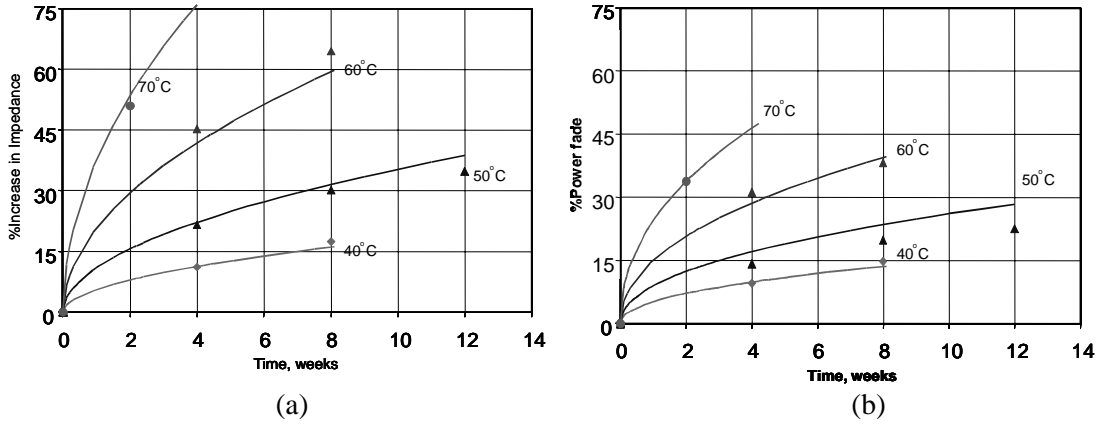


Fig. 5. (a) Percent Increase in impedance and (b) Percent power fade for Group A calendar life cells at 60% SOC. Markers represent the experimental values.

The fact that both impedance and power change with  $(\text{time})^{1/2}$  implies that the data follow either one-dimensional kinetics or some other mechanism that has  $(\text{time})^{1/2}$  dependency. In the literature, one process for thin-film growth describes kinetics as having  $(\text{time})^{1/2}$  dependence. Applying these concepts to the lithium-ion battery, growth of the thin-film, solid electrolyte interface (SEI) layer may be the cause of the observed effect [6,7]. Based on the data from this study, we do not know on which electrode the SEI layer is growing. However, based on literature reports [8], we think it is the SEI layer on the cathode that makes the largest contribution to the observed changes.

### 3.1.2. Cycle Life

The plots of impedance versus cell voltage and power versus cell voltage are very similar to those shown in Figs. 3 and 4. Indeed, the trends in the impedance increase and power fade are analogous.

The fitting parameters for the SOC and  $\Delta$ SOCs are given in Table 5. From these data, the value of  $z$  in Eq. 1 for the impedance at a given SOC is strongly dependent on the  $\Delta$ SOC. At 60% SOC and 3%  $\Delta$ SOC, the  $z$  value is approximately 0.50; while at 6%  $\Delta$ SOC, it is approximately 0.10. In the case of power fade, at 60% SOC, there is also a marked change in

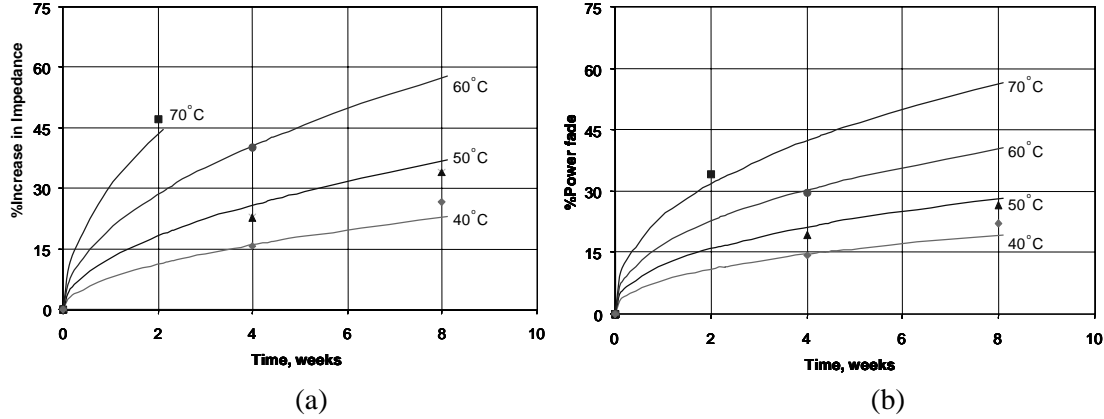


Fig. 6. (a) Percent increase in impedance and (b) Percent power fade for Group B calendar life cells at 60% SOC. Markers represent the experimental values.

mechanism from 3% to 6%  $\Delta$ SOC, as indicated by the values of  $z$ . The situation at 80% SOC is not as clear-cut. The values of  $z$  at 3% and 6%  $\Delta$ SOC, 0.19 and 0.14, respectively, are not statistically different from one another, and hence may be the same.

As discussed in the calendar life section, a  $z$  value of 0.5 may indicate one-dimensional diffusion kinetics or SEI layer growth. The lower values of  $z$  indicate that a different mechanism than film growth inversely proportional to film thickness is causing ASI increases. Possible alternative mechanisms coming into play are the dissolution of the SEI with time, a separate reaction of the PVDF binder with the electrodes, or the reaction of  $\text{LiPF}_6$  with the electrodes and/or electrolyte [9].

Table 5. Fitting Parameters from Cycle Life Study

SOC, %	$\Delta$ SOC, %	Impedance Increase					Power Fade			
			$z$	$E_a/R$ , K	$\ln A$	$r^2$	$z$	$E_a/R$ , K	$\ln A$	$r^2$
60	3	Value	0.54	3414.94	13.52	0.98	0.25	2079.32	9.49	1.00
		Std error	0.09	368.24	1.03		0.00	1.99	0.01	
	6	value	0.11	1881.29	9.48	0.94	0.08	1330.07	7.46	0.92
		std error	0.08	378.44	1.09		0.07	306.43	0.89	
80	3	value	0.57	4648.37	17.19	0.96	0.19	2940.95	12.17	0.99
		std error	0.12	566.63	1.63		0.14	396.34	1.09	
	6	value	0.15	2317.42	10.84	0.91	0.14	1739.50	8.74	0.91
		std error	0.10	487.42	1.40		0.07	341.04	0.98	

### 3.2. Gen 2

The Gen 2 cells had a significantly better performance and longer life than those of Gen 1. The initial average values from the HPPC characterization test for impedance and power were 32.7 m $\Omega$  and 67.7 W, respectively, as opposed to those of Gen 1 cells (59.1 m $\Omega$  and 36.1 W, Table 3). In our analysis of the HPPC data, some distinct differences in dependence on time were seen.

#### 3.2.1. Calendar Life

A plot of discharge area-specific impedance versus time is given in Fig. 7, showing the data from the experiments at 45 and 55°C. Fig. 7. also includes the calculated increase in discharge area-specific



impedance for Gen 1 cells. From this figure, it can clearly be seen that the rate of impedance rise in the Gen 2 cells is much lower than that in the Gen 1 cells.

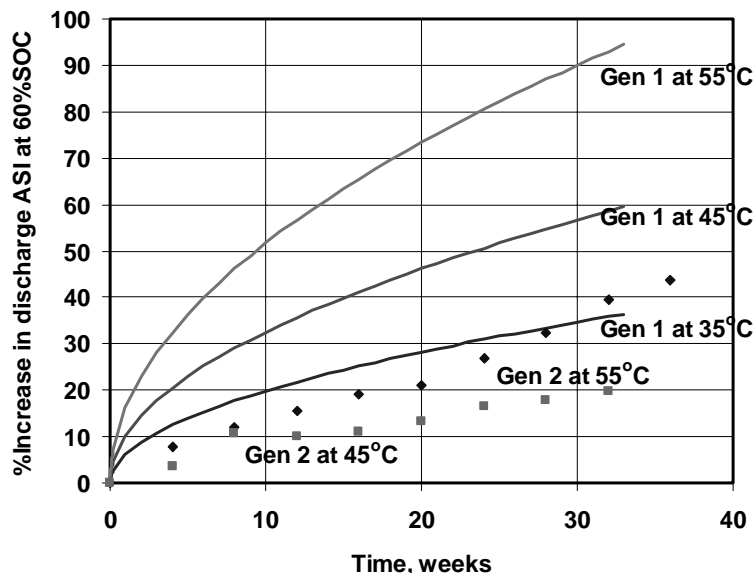


Fig. 7. Percent increase in discharge impedance as a function of time and temperature. The calculated values for the Gen 1 cells are represented by the solid curves, and the values for Gen 2, by markers.

The form of the equation used for fitting of Gen 2 calendar life data depended on temperature (Fig. 8). At 25°C, a straight-line fit produced a very high value of the regression coefficient,  $r^2$ , 0.99. At 45°C, the data were fit by a  $t^{1/2}$  curve with an adequate value of  $r^2$ , 0.94. However, at 55°C, the value of  $r^2$  dropped to a low value of 0.87. Another way to look at the 45 and 55°C data is to divide them into two regions, parabolic and linear (see Fig. 9).

In the literature, the growth of a thin film, e.g., SEI layer, can be proportional to  $(\text{time})^{1/2}$ . Square-root-of-time dependent (parabolic kinetics), as well as linear-with-time, mechanisms have been found for the growth of an oxide film on a metal surface [10–15]. The square-root-of-time dependent mechanisms tend to have a strong thermal diffusion component and follow Arrhenius kinetics. In the linear-with-time case, the rate of oxidation is constant with time and is thus independent of the amount of gas or metal previously consumed in the formation of the oxide layer. The linear growth law is found to describe metal oxidation reactions whose rate is controlled by a surface reaction step or by diffusion of one of the reactants to the surface of the metal.

Applying this analogy to the Li-ion battery case, the formation of a thin film on a Li-ion battery electrode may occur in much the same manner as an oxide film on a metal. It is possible that the reaction of the electrolyte with an electrode to form species such as lithium alkoxides, lithium carbonates or LiF follows parabolic kinetics. For the linear section, the reaction mechanism and/or products may have changed. Another possibility is that the surface film no

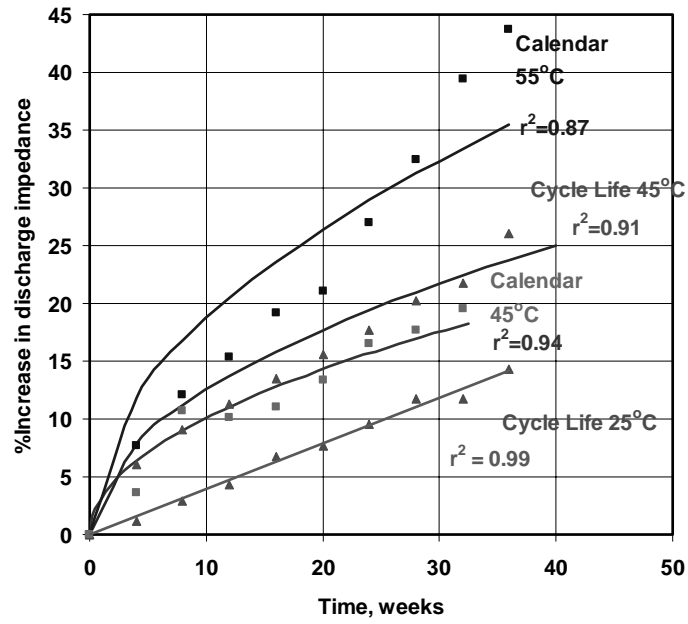


Fig. 8. Initial fits of the Gen 2 impedance increase data.

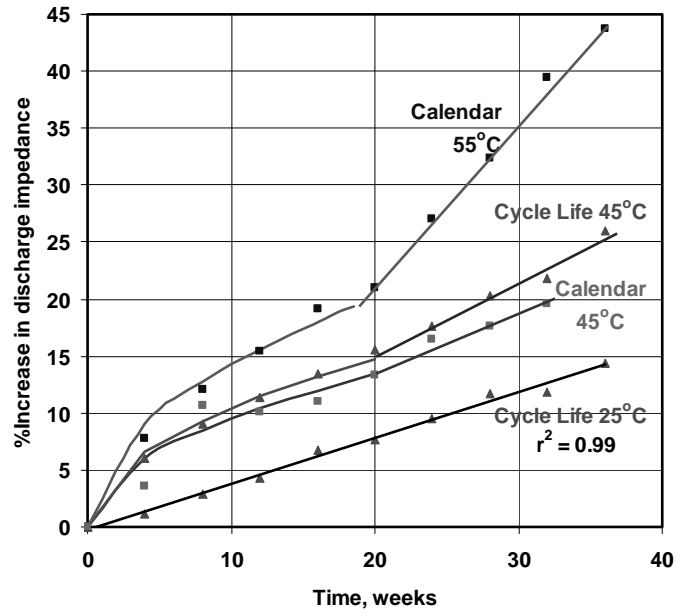


Fig. 9. Data from 45 and 55°C Gen 2 cell tests divided into two regions, parabolic and linear.

longer protects the electrode surface. These types of behaviors have been reported in the literature of the oxidation of Fe [16], Nb [17,18], and Ce [19].

### 3.2.2. Cycle Life

Plots of the increase in discharge impedance with time are given in Figs. 8 and 9 for the two temperatures, 25 and 45°C. The plots show that the mechanism of impedance increase is sensitive to temperature. The impedance increase at 25°C appears to be linear with time, while that at 45°C follows the pattern described under calendar life. Indeed, there is very little difference between the calendar and cycle life data at 45°C.

The idea of parabolic and linear regions may also be used to rationalize the 25°C data. In any reaction following parabolic kinetics, the initial rates appear linear. The apparent linearity of the data at 25°C may indicate that the reaction has not progressed sufficiently to display parabolic behavior.

As discussed in the calendar life section under Gen 2, there are many possible mechanisms for impedance increase. Which exact mechanism is the dominant one depends on temperature, test conditions and cell chemistry. The delineation of the exact mechanism or mechanisms is the subject of ongoing, intense research as part of the ATD Program.

## 4. Conclusions

In Gen 1 calendar life experiments, useful cell life was strongly affected by temperature and time. Increased temperature accelerated cell performance degradation. The rates of impedance increase and power fade followed simple laws based on a power of test time and Arrhenius kinetics. The data have been modeled using these two concepts and the calculated data agree well with the experimental values.

The Gen 1 calendar life impedance increase and power fade data follow  $(\text{time})^{1/2}$  kinetics. This may be due to SEI layer growth. From the cycle life experiments, the impedance increase data follow  $(\text{time})^{1/2}$  kinetics also, there is an apparent change in overall power fade mechanism from 3% to 6%  $\Delta\text{SOC}$ . Here, the power of time changes to a value less than 1/2 and indicates that the power fade mechanism is more complex than SEI layer growth.

The Gen 2 calendar and cycle life impedance increase data follow either “linear” or  $(\text{time})^{1/2}$  plus linear kinetics, depending on time and temperature. Temperature dependence on kinetic law was also found in the cycle life data.

## 5. Acknowledgment

This work was performed under the auspices of the U.S. Department of Energy, Office of Advanced Automotive Technologies, under Contract No. W-31-109-Eng-38.

## 6. References

- [1] I. Bloom, B. W. Cole, J. J. Sohn, S. A. Jones, E. G. Polzin, V. S. Battaglia, G. L. Henriksen, C. Motloch, R. Richardson, T. Unkelhaeuser and H. L. Case, *J. Power Sources* **101** (2001) 238–247.
- [2] C. G. Motloch, I. Bloom, and T. Unkelhaeuser, Gen 1: Cell Development and Testing; Overview of ATD Gen 1 Cell Performance and Life Evaluations, FY 2000 Progress Report for the Advanced Technology Development Program, U.S. Department of Energy, Office of Advanced Automotive Technologies, December 2000.
- [3] C. Motloch, J. Christophersen, R. Wright, Richardson, C. Ho, D. Glenn, K. Gering, T. Murphy, I. Bloom, S. Jones, V. Battaglia, G. Henriksen, R. Jungst, H. Case, T. Unkelhaeuser, and D. Doughty, Overview of ATD Gen 2 Cell Performance and Life Evaluations, U.S. Department of Energy, Office of Advanced Automotive Technologies, FY 2001 Progress Report for the Advanced Technology Development Program

- [4] PNGV Battery Test Manual, DOE/ID-10597, Rev. 3, February 2001.
- [5] Raymond A. Sutula, et al., FY 2000 Progress Report for the Advanced Technology Development Program, U.S. Department of Energy, Office of Advanced Automotive Technologies, December 2000.
- [6] E. Strauss, D. Golodnitsky, and E. Peled, *Electrochemical and Solid State Letters*, **2** (1999) 115-117.
- [7] G. Blomgren, *J. Power Sources*, **81-82** (1999) 112-118.
- [8] K. Amine, M. J. Hammond, J. Liu, C. Chen, D. W. Dees, A. N. Jansen, and G. L. Henriksen, Proc. of the 10<sup>th</sup> Int. Meeting on Lithium Batteries, Como, Italy, May 28-June 2, 2000, p. 332 (2000).
- [9] See E. Peled, D. Golodnitsky, C. Menachem, and D. Bar-Tow, *J. Electrochem. Soc.*, **145**, (1998) 3482–3486 for a more complete discussion of the types of reactions that can occur in a lithium-ion battery.
- [10] N. Birks and G. H. Meier, Introduction to High Temperature Oxidation of Metals, Edward Arnold Ltd., London, 1983.
- [11] Per Kofstad, High-Temperature Oxidation of Metals, John Wiley and Sons, New York, 1966.
- [12] K. Hauffe, Oxidation of Metals, Plenum Press, New York, 1965.
- [13] W. Jost, Diffusion in Solids, Liquids and Gases, 3<sup>rd</sup> Printing, Addendum, Academic Press, Inc., New York, 1960.
- [14] J. Crank, The Mathematics of Diffusion, 2<sup>nd</sup> edition, Clarendon Press, Oxford, 1975.
- [15] Per Kofstad, Nonstoichiometry, Diffusion, and Electrical Conductivity in Binary Metal Oxides, John Wiley and Sons, New York, 1972.
- [16] D. W. Juenker, R. A. Muessner and C. E. Birchenall, *Corrosion*, **14** (1958) 57-64.
- [17] T. Hurlen, *J. Institute of Metals*, **89** (1960-61) 273-280.
- [18] B. Cox and T. Johnston, *Trans. Met. Soc. AIME*, **227** (1963) 36-47.
- [19] J. Loriers, *Comptes rendus*, **229** (1949) 547-549.

## 7. Affiliation



**Dr. Ira Bloom**

Electrochemical Technology Program  
Argonne National Laboratory  
9700 South Cass Avenue  
Argonne, IL 60439  
Tel: 630-252-4516 Fax: 630-252-4716  
e-mail: [bloom@cmt.anl.gov](mailto:bloom@cmt.anl.gov)  
Manager, Electrochemical Analysis and Diagnostics Laboratory



**Mr. Scott A. Jones**

Electrochemical Technology Program  
Argonne National Laboratory  
9700 South Cass Avenue  
Argonne, IL 60439  
Tel: 630-252-9894 Fax: 630-252-4716  
e-mail: [jones@cmt.anl.gov](mailto:jones@cmt.anl.gov)  
Test Engineer



**Dr. Vincent S. Battaglia**

Argonne National Laboratory  
Washington, DC  
Tel: 202-488-2461 Fax: 202-488-24113  
e-mail: [batman@anl.gov](mailto:batman@anl.gov)  
Technical Coordinator



**Mr. Edward G. Polzin**

Electrochemical Technology Program  
Argonne National Laboratory  
9700 South Cass Avenue  
Argonne, IL 60439  
Tel: 630-252-1213 Fax: 630-252-4716  
e-mail: [polzin@cmt.anl.gov](mailto:polzin@cmt.anl.gov)  
Test Engineer



**Mr. Gary L. Henriksen**

Electrochemical Technology Program  
Argonne National Laboratory  
9700 South Cass Avenue  
Argonne, IL 60439  
Tel: 630-252-4591 Fax: 630-252-4716  
e-mail: [henriksen@cmt.anl.gov](mailto:henriksen@cmt.anl.gov)  
Manager, Battery Technology Department



**Dr. Chester G. Motloch**

Idaho National Engineering and Environmental Laboratory  
P.O. Box 1625  
Idaho Falls, ID 83415  
Tel: 208-526-0643 Fax: 208-526-0969  
e-mail: [motlchg@inel.gov](mailto:motlchg@inel.gov)  
Consulting Engineer



**Mr. Jon P. Christophersen**

Idaho National Engineering and Environmental Laboratory  
P.O. Box 1625  
Idaho Falls, ID 83415  
Tel: 208-526-4280 Fax: 208-526-0969  
e-mail: [chrijp@inel.gov](mailto:chrijp@inel.gov)  
Engineer



**Mr. Jeffery R. Belt**

Idaho National Engineering and Environmental Laboratory  
P.O. Box 1625  
Idaho Falls, ID 83415  
Tel: 208-526-3813 Fax: 208-526-0969  
e-mail: [beltjr@inel.gov](mailto:beltjr@inel.gov)  
Senior Engineer



**Dr. Randy B. Wright**

Idaho National Engineering and Environmental Laboratory  
P.O. Box 1625  
Idaho Falls, ID 83415  
Tel: 208-526-0959 Fax: 208-526-0969  
e-mail: [rbw2@inel.gov](mailto:rbw2@inel.gov)  
Advisory Scientist



**Mr. Chin D. Ho**

Idaho National Engineering and Environmental Laboratory  
P.O. Box 1625  
Idaho Falls, ID 83415  
Tel: 208-526-3297 Fax: 208-526-1400  
e-mail:  
Test Engineer



**Dr. Rudolph G. Jungst**

Sandia National Laboratories  
P.O. Box 5800  
Albuquerque, NM 87185  
Tel: 505-1103 Fax: 505-844-6972  
e-mail: [rgjunst@sandia.gov](mailto:rgjunst@sandia.gov)



**Mr. Herbert L. Case**

Sandia National Laboratories  
P.O. Box 5800  
Albuquerque, NM 87185  
Tel: 505-284-3024 Fax: 505-844-6972  
e-mail: [hlcase@sandia.gov](mailto:hlcase@sandia.gov)  
Test Engineer



**Dr. Daniel H. Doughty**

Sandia National Laboratories  
P.O. Box 5800  
Albuquerque, NM 87185  
Tel: 505-844-8105 Fax: 505-844-6972  
e-mail: [dhdough@sandia.gov](mailto:dhdough@sandia.gov)  
Manager, Li-Battery Section